Title

Preserving Vascular Integrity Protects Mice against Multidrug-Resistant Gram-Negative Bacterial Infection.

Permalink

Journal

ISSN

Authors

Gebremariam, Teclegiorgis
Zhang, Lina
Alkhazraji, Sondus
et al.

Publication Date

2020-07-22

DOI

Peer reviewed

Preserving Vascular Integrity Protects Mice against Multidrug-Resistant Gram-Negative Bacterial Infection

Teclegiorgis Gebremariam,[a] Lina Zhang,[a,b] Sondus Alkhazraji,[a] Yiyou Gu,[a] Eman G. Youssef,[a,c] Zongzhong Tong,[d] Erik Kish-Trier,[d] Ashok Bajji,[d] Claudia V. de Araujo,[e] Bianca Rich,[e] Samuel W. French,[a,f] Dean Y. Li,[d,e,g,h]* Alan L. Mueller,[d] Shannon J. Odelberg,[e] Weiquan Zhu,[e] [ORCID] Ashraf S. Ibrahim[a,f]

[a]The Lundquist Institute for Biomedical Innovations at Harbor-University of California Los Angeles (UCLA) Medical Center, Torrance, California, USA
[b]College of Wildlife Resources, Northeast Forestry University, Harbin, China
[c]Faculty of Postgraduate Studies for Advanced Sciences, Beni-Suef University, Beni-Suef, Egypt
[d]A6 Pharmaceuticals, Salt Lake City, Utah, USA
[e]Department of Internal Medicine, University of Utah, Salt Lake City, Utah, USA
[f]David Geffen School of Medicine at UCLA, Los Angeles, California, USA
[g]Department of Human Genetics, University of Utah, Salt Lake City, Utah, USA
[h]Department of Oncological Sciences, University of Utah, Salt Lake City, Utah, USA

ABSTRACT The rise in multidrug-resistant (MDR) organisms portends a serious global threat to the health care system with nearly untreatable infectious diseases, including pneumonia and its often fatal sequelae, acute respiratory distress syndrome (ARDS) and sepsis. Gram-negative bacteria (GNB), including *Acinetobacter baumannii*, *Pseudomonas aeruginosa*, and carbapenemase-producing *Klebsiella pneumoniae* (CPKP), are among the World Health Organization's and National Institutes of Health's high-priority MDR pathogens for targeted development of new therapies. Here, we show that stabilizing the host's vasculature by genetic deletion or pharmacological inhibition of the small GTPase ADP-ribosylation factor 6 (ARF6) increases survival rates of mice infected with *A. baumannii*, *P. aeruginosa*, and CPKP. We show that the pharmacological inhibition of ARF6-GTP phenocopies endothelium-specific *Arf6* disruption in enhancing the survival of mice with *A. baumannii* pneumonia, suggesting that inhibition is on target. Finally, we show that the mechanism of protection elicited by these small-molecule inhibitors acts by the restoration of vascular integrity disrupted by GNB lipopolysaccharide (LPS) activation of the TLR4/MyD88/ARNO/ARF6 pathway. By targeting the host's vasculature with small-molecule inhibitors of ARF6 activation, we circumvent microbial drug resistance and provide a potential alternative/adjunctive treatment for emerging and reemerging pathogens.

KEYWORDS *Acinetobacter baumannii*, *Pseudomonas aeruginosa*, *Klebsiella pneumoniae*, ARF6, LPS, drug resistance, sepsis, Gram-negative bacteria, lipopolysaccharide, multidrug resistance, vascular permeability

Current global trends in healthcare-associated infections (HAIs) are characterized by the emergence and reemergence of multidrug-resistant (MDR) pathogens (1). There are ~1.0 million HAIs in the United States each year, which cause 70,000 to 100,000 deaths and $30 billion in costs (2). Gram-negative bacteria (GNB) are responsible for half of all HAIs. In particular, *Acinetobacter baumannii*, *Pseudomonas aeruginosa*, and carbapenemase-producing *Klebsiella pneumoniae* (CPKP) have emerged as predominant causes of MDR HAIs (3, 4). Some strains of these pathogens are resistant to all FDA-approved antibiotics and, in many cases, lead to serious complications (e.g., sepsis [5]), which are associated with high mortality and morbidity rates (6–8). Sepsis

Address correspondence to Ashraf S. Ibrahim, ibrahim@lundquist.org.

* Present address: Dean Y. Li, Merck & Co, Inc., Kenilworth, New Jersey, USA.

results from a dysregulated host immune response associated with the production of a cytokine storm, which contributes to increased vascular permeability, tissue edema, organ failure, and death (9–12).

Evidence from the past few decades shows that the development of resistance to antibiotics is inevitable. Thus, it is essential that we develop novel treatments that do not rely solely on antibacterial action. Altering the patient's own host response is one such alternative strategy for combating infectious diseases. Stabilizing the vasculature to prevent fluid leak, without compromising the beneficial innate immune system response, may allow the host ample time to clear the infection without causing organ failure. The activation state of ARF6, which is a convergence point in the signaling pathways of several inflammatory mediators and cytokines, plays a major role in controlling vascular permeability (13–16). When ARF6 is in its activated GTP-bound state, permeability is increased, and when it is in its inactive GDP-bound state, the vasculature is stabilized, leading to decreased permeability. Proinflammatory agonists, such as interleukin-1β (IL-1β), GNB lipopolysaccharides (LPS), and vascular endothelial growth factor (VEGF), activate ARF6, which, in turn, promotes the internalization of the adherens junction protein vascular endothelial (VE)-cadherin and thereby increases endothelial permeability (13, 15, 16). We have shown that stabilizing the vasculature by reducing ARF6 activity is an effective strategy for reversing pathology and increasing survival rates in several preclinical models of inflammatory and vascular disease, including arthritis (15), LPS-induced endotoxemia (13), and diabetic retinopathy (16). Here, we show that stabilizing the vasculature through pharmacological inhibition of ARF6 activation by small molecules can increase survival rates and reduce pathology in preclinical models of MDR GNB infections.

(This work was presented in part at ASM Microbe, 16 to 20 June 2016, and at the 2nd International Symposium on Alternative to Antibiotics [ATA], 12 to 15 December 2016.)

RESULTS AND DISCUSSION

***Arf6* conditional knockout mice are resistant to *A. baumannii* pneumonia.** Mice infected with MDR *A. baumannii* die from endotoxemia caused by LPS activation of Toll-like receptor-4 (TLR4), since TLR4-deficient mice are completely protected from *A. baumannii* bacteremia (17). We hypothesized that the triggering of TLR4 by LPS during *A. baumannii* infection leads to the activation of ARF6, resulting in increased virulence by compromising vascular integrity. To test this hypothesis, we compared the virulence of *A. baumannii* HUMC1 (a strain resistant to all antibiotics except colistin) (18, 19) in *Arf6*$^{f/+}$ versus *Arf6* conditional knockout mice using pulmonary infection. *Arf6* conditional knockout mice were significantly more resistant to *A. baumannii* pneumonia, with 40% overall survival after 21 days postinfection versus 0% survival for mice carrying two active *Arf6* alleles (*Arf6*$^{f/+}$) (Fig. 1A). In another study, *Arf6*$^{f/+}$ or *Arf6* conditional knockout mice (*Arf6*$^{f/-}$;+/*Tie2-cre*) were infected with *A. baumannii* via inhalation and sacrificed for lung bacterial burden 4 days postinfection. *Arf6* knockout mice had ~1.5-log$_{10}$ lower *A. baumannii* burden than *Arf6*$^{f/+}$ mice (Fig. 1B). Collectively, these studies suggest that the disruption of endothelial cell ARF6 allows the mouse immune system the opportunity to clear *A. baumannii* infection.

To test whether the enhanced resistance of *Arf6* knockout mice to *A. baumannii* pneumonia is due to the enhanced vascular integrity of the lungs, we infected mice with *A. baumannii* as described above and 3 days later intravenously injected them with Evans blue dye to assess lung permeability. As expected, *Arf6*$^{f/+}$ mice showed vascular permeability increased by ~25% compared to that of *Arf6* conditional knockout mice (Fig. 1C). Histopathological examination of the lungs corroborated the permeability results, with *Arf6*$^{f/+}$ mouse lungs demonstrating enhanced tissue edema with extensive hemorrhage compared to lungs of *Arf6* conditional knockout mice (Fig. 1D).

ARF6 inhibitors are protective against murine bacterial pneumonia. Because ARF6 activation promotes the virulence of *A. baumannii*, we hypothesized that pharmacologic ARF6 inhibition can be used to target GNB infections by stabilizing the vasculature. Thus, we tested whether the pharmacologic inhibition of ARF6 could
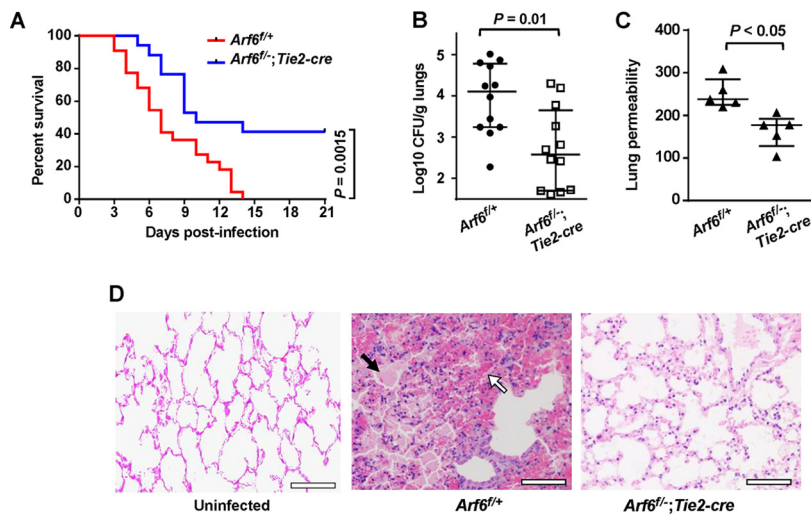
FIG 1 Endothelial cell *Arf6* deletion increases survival rates and reduces disease severity due to MDR *A. baumannii* pneumonia. (A) Survival of *Arf6*$^{f/+}$ mice (n = 22) or endothelial cell ARF6 null mice (*Arf6*$^{f/-}$; *Tie2-cre*) (n = 17) with *A. baumannii* pneumonia. (B) Lung bacterial burden (n = 12/arm); (C) lung permeability; (D) histopathological examination of lungs stained with H&E and harvested from *Arf6*$^{f/+}$ or endothelial cell ARF6 null mice 4 days postinfection with *A. baumannii* via inhalation. Lungs from uninfected *Arf6*$^{f/+}$ mice are included as a control. Black and white arrows in panel D denote tissue edema and hemorrhage in *Arf6*$^{f/+}$ mice, respectively. Bars are 20 μM. Data shown in panels B and C are presented as the medians ± interquartile ranges.

increase the survival of mice with MDR GNB pneumonia. Small-molecule ARF6 inhibitors NAV-2729 (structure and method of synthesis were previously described in Yoo et al. [20]), A6-4424, and its prodrug, A6-5093 (see Fig. S1A in the supplemental material), were evaluated for efficacy in treating murine pneumonia due to GNB. NAV-2729 (50% inhibitory concentration [IC$_{50}$] of 1.5 μM) has been shown to have therapeutic benefit in alleviating animal models of diabetic retinopathy (16). A6-5093 is a new, highly soluble prodrug of A6-4424 designed to enhance *in vivo* administration (see the supplemental material for the synthesis of A6-4424 and A6-5093). When A6-5093 is administered *in vivo*, its lysyl group is rapidly cleaved to produce A6-4424 (Fig. S1A), an active ARF6 inhibitor with an IC$_{50}$ of 1.9 μM (Fig. S1B and C).

Immunosuppressed mice were infected with aerosolized *A. baumannii* HUMC1 (a virulent MDR strain of *A. baumannii* to which immunocompetent mice are resistant) (18, 19). Mice were treated daily for 7 days with (i) 30 mg/kg of body weight NAV-2729 or A6-4424 (both dissolved in dimethylacetamide/polyethylene glycol [DMA/PEG] and the dose chosen based on pharmacokinetic [PK] data shown in Fig. S1D to G), (ii) 43 mg/kg A6-5093 (dissolved in saline and equivalent to 30 mg/kg A6-4424), (iii) DMA/PEG (vehicle), or (iv) 2.5 mg/kg colistin twice a day (b.i.d.). Vehicle-treated mice had a median survival time of 8 days and almost complete mortality by day 15 postinfection. In contrast, NAV-2729 or A6-5093 enhanced median survival time to >21 days, with an overall survival of >80% by day 21 postinfection (Fig. 2A). Although mice treated with A6-4424 had a median survival time similar to that of vehicle-treated mice, 21-day survival was 50% versus 5% in vehicle-treated mice. Interestingly, the enhanced survival of mice seen with the ARF6 inhibitors far exceeded survival seen with the current first-line therapy of colistin (Fig. 2A).

We investigated if the survival benefit correlated with the reduction of bacterial burden in the lungs. Mice were infected and treated as described above and sacrificed on day 4 postinfection. Mice treated with NAV-2729 or A6-5093 had at least a 1-log$_{10}$ reduction in lung bacterial burden compared to that of vehicle-treated mice (Fig. 2B). Since *A. baumannii* HUMC1 is colistin sensitive (19), mice treated with colistin had a 2-log$_{10}$ reduction of lung bacterial burden versus vehicle-treated mice and 1-log$_{10}$ reduction versus ARF6 inhibitors (Fig. 2B). Thus, the decreased efficacy of colistin in survival studies is likely attributable to its toxicity (21).
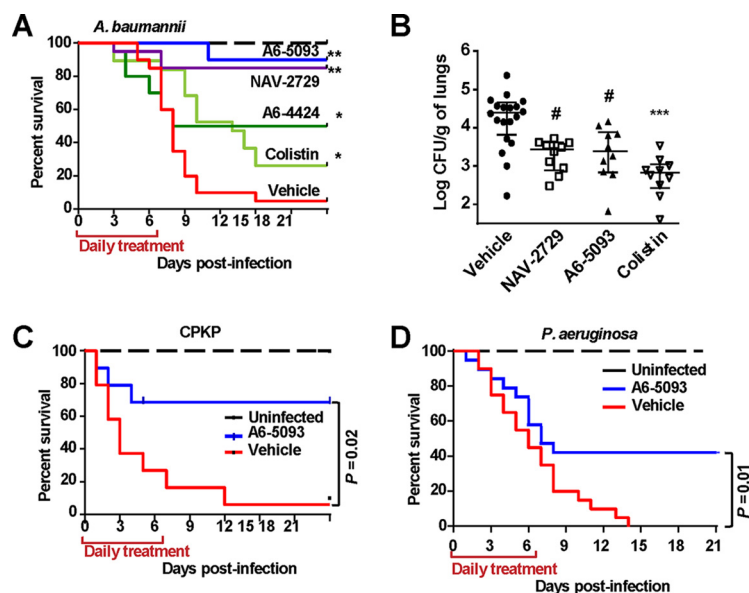
FIG 2 Pharmacologic inhibition of ARF6 increases survival rates and reduces disease severity due to MDR GNB infection. ARF6 inhibitors (A6-5093, NAV-2729, and A6-4424) increase survival ($n = 20$ mice for all groups, except those for A6-5093 [10 mice] and colistin [19 mice]) (A) and reduce lung bacterial burden (B) of immunosuppressed mice (200 mg/kg i.p. cyclophosphamide and 250 mg/kg subcutaneous corti-sone acetate given on days −2 and +3 relative to infection) with MDR *A. baumannii* pneumonia. Lungs were harvested on day +4 relative to infection. *, $P < 0.05$ versus vehicle-treated mice; **, $P < 0.02$ versus all others in panel A; #, $P < 0.05$ versus vehicle-treated mice; ***, $P < 0.03$ versus all others in panel B. (C and D) ARF6 inhibitors increase survival rate of immunosuppressed mice infected with MDR CPKP ($n = 10$/group) (C) or MDR *P. aeruginosa* ($n = 20$/group) (D). Log rank test for all analyses of survival and Wilcoxon rank sum test for lung bacterial burden.

We also evaluated the activity of A6-5093 against murine pneumonia caused by MDR *P. aeruginosa* or CPKP. Mice infected with CPKP or *P. aeruginosa* and treated with A6-5093 had 70% and 45% 21-day survival rates versus 10% and 0% survival rates for vehicle-treated mice, respectively (Fig. 2C and D). Collectively, these results confirm the protective activity of ARF6 inhibitors against at least three MDR GNB, which are noted for causing HAI (22).

ARF6 inhibitors enhance vascular integrity without affecting inflammation. We investigated the mechanism by which ARF6 inhibitors protect from GNB infection. First, we determined if any of our ARF6 inhibitors has a direct inhibitory or microbicidal effect on the three MDR bacteria under study. We performed MIC testing of the pathogen using NAV-2729, A6-4424, or vehicle control before and after using the bacteria in infection models. We observed no difference in *A. baumannii*, CPKP, or *P. aeruginosa* growth even at concentrations of 156 μM (data not shown), thereby indicating that the *in vivo* protection is due to an effect of the inhibitors on the host.

ARF6 activation leads to increased vascular permeability via internalization of the adherens junction protein VE-cadherin (13, 15, 16). Thus, we hypothesized that ARF6 inhibitors protect mice from GNB infection by maintaining vascular integrity. To investigate this possibility, we determined the effect of ARF6 inhibitors on *in vivo* organ permeability and the inflammatory response to *A. baumannii* pneumonia. Mice with *A. baumannii* pneumonia had an ~50% and 30% increase in lung and kidney permeability, respectively, compared to uninfected mice. Treatment with either NAV-2729 or A6-5093 reduced the *A. baumannii*-mediated vascular permeability of lungs and kidneys to levels seen with uninfected mice (Fig. 3A). These results were corroborated by histological examination of lungs harvested from mice infected with *A. baumannii*, which showed signs of pneumonia and tissue edema consistent with increased vascular permeability. Lungs harvested from mice infected and treated with either NAV-2729 or colistin showed more normal architecture with minimal to no signs of tissue edema
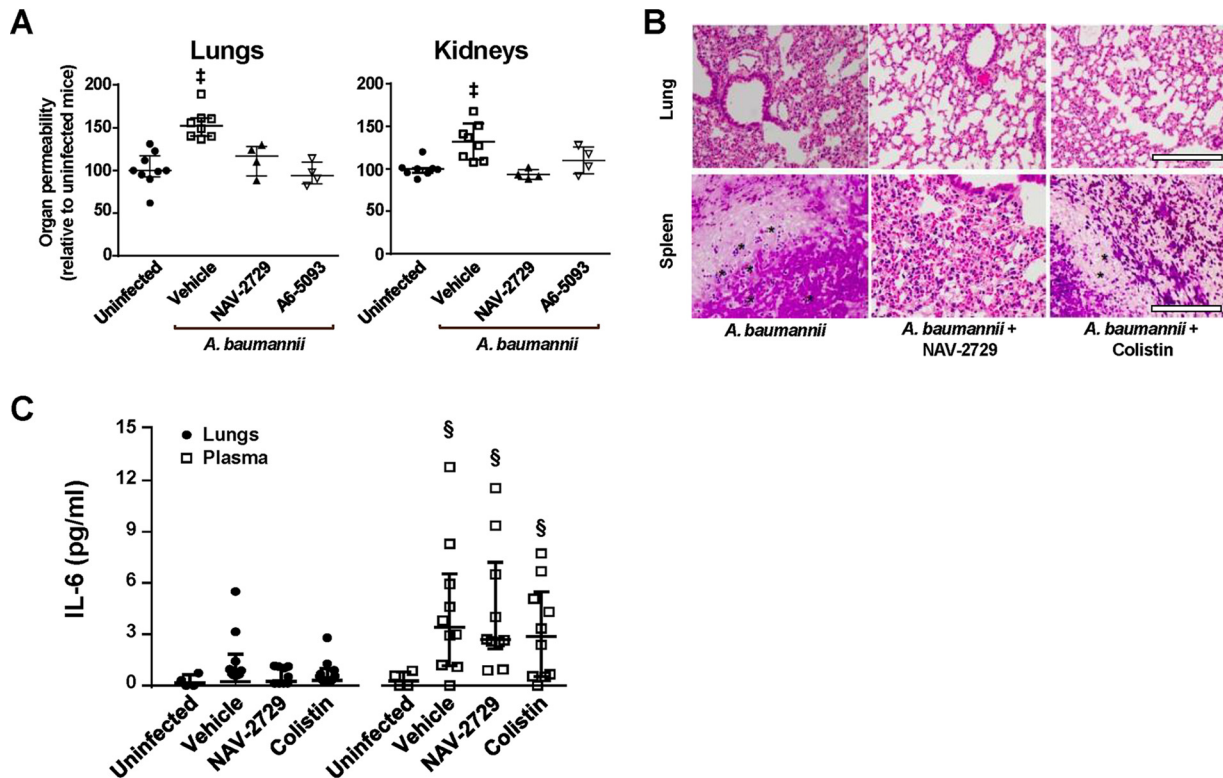
FIG 3 ARF6 inhibition reduces organ permeability and disease severity without affecting the inflammatory response to *A. baumannii* pneumonia. (A) ARF6 inhibitors (NAV-2729 and A6-5093) decreased permeability in the lungs and kidneys of *A. baumannii* HUMC1-infected mice. ‡, $P < 0.05$ versus other treatments. (B) NAV-2729 (30 mg/kg) reduced severity of *A. baumannii* infection, as shown by histopathological examination of lungs with H&E stain and spleen with Gram stain. An asterisk denotes necrobiosis in spleen harvested from vehicle-treated mice and, to a lesser extent, colistin-treated mice, but not from mice treated with NAV-2729. Bars represent 100 μM. (C) IL-6 levels in lungs and plasma of *A. baumannii* HUMC1-infected mice and treated with vehicle control, NAV-2729, or colistin. §, $P < 0.02$ versus uninfected mice. Organs of neutropenic mice were harvested on day +3 (A) and day +4 (B and C) relative to infection. Data in panels A and C are presented as the medians ± interquartile ranges.

(Fig. 3B). Necrobiosis was evident in spleens taken from *A. baumannii*-infected mice without treatment or with those treated with colistin but not in spleens harvested from infected mice and treated with NAV-2729 (Fig. 3B). The observed necrosis in spleens from colistin-treated mice is likely attributable to the toxicity of colistin (21).

LPS-induced endotoxemia results in a robust immune response via TLR4-mediated NF-κB activation (17). To determine the effect of ARF6 inhibitors on the inflammatory immune response to *A. baumannii* pneumonia, we infected immunosuppressed mice and treated them as described above for 4 days. Mice were sacrificed, and plasma and lungs were collected for the determination of inflammatory cytokines. Due to the immunosuppression, which results in ~9 days of leukopenia (23), only IL-6 was detectable. No differences in IL-6 levels were observed in the lungs or plasma collected from vehicle-, NAV-2729-, or colistin-treated mice (Fig. 3C). Collectively, these results suggest that ARF6 inhibitors protect mice from *A. baumannii* pneumonia by preserving vascular integrity without affecting the inflammatory immune response.

Bacterial LPS induces vascular permeability via the MyD88/ARNO/ARF6-GTP pathway. Previously, we showed that TLR4 activation by LPS compromises vascular integrity via the activation of the MyD88/ARNO/ARF6 pathway (13). It was also shown that lethality in mice infected with *A. baumannii* is mainly determined by the ability of the bacteria to activate TLR-4 through shed LPS (17). We hypothesized that GNB induces vascular permeability by the activation of the MyD88/ARNO/ARF6 pathway through their LPS. To investigate this hypothesis, we studied if *A. baumannii* and its LPS induce human umbilical vein endothelial cell (HUVEC) vascular permeability *in vitro*. The virulent *A. baumannii* MDR HUMC1 and its cell-free supernatant (this strain sheds LPS [17]) induced HUVEC permeability equivalent to that seen with commercially
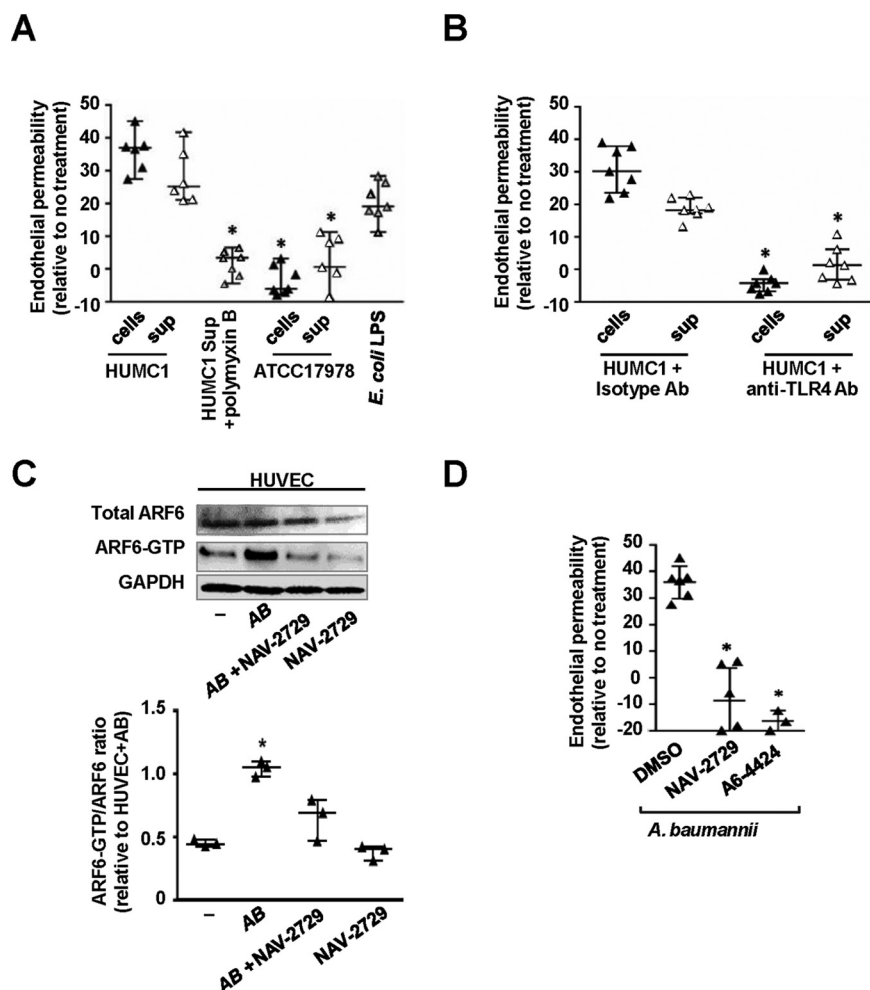
FIG 4 *A. baumannii*-mediated HUVEC permeability is induced by LPS-TLR4 signaling through ARF6. (A) *A. baumannii* HUMC1 (virulent MDR) cells and supernatants (sup) induce HUVEC permeability to a level similar to that of *E. coli* LPS. Removing LPS by polymyxin B blocks this induction. ATCC 17978 (avirulent, drug-sensitive) cells and supernatants do not induce permeability. *, $P < 0.005$ versus HUMC1, HUMC1 supernatant, or *E. coli* LPS. (B) A permeability assay was conducted with HUMC1 or its supernatant in the presence of 50 μg/ml anti-TLR4 or isotype-matched control antibodies (Ab). *, $P < 0.001$ versus isotype-matched antibody. (C) ARF6-GTP pulldown assays show that *A. baumannii* HUMC1 (AB) induces ARF6 activation and NAV-2729 blocks it. Quantification of the ARF6-GTP/total ARF6 ratio by densitometer (3 independent experiments) shows *A. baumannii* induces endothelial cell ARF6 activation 2-fold, while NAV-2729 inhibits this activation. *, $P < 0.05$ versus all other comparators. GAPDH, glyceraldehyde-3-phosphate dehydrogenase. (D) A HUVEC permeability assay was conducted with HUMC1 in the presence of 50 μM ARF6 inhibitor (NAV-2729 or A6-4424). *, $P < 0.0015$ versus HUMC1 cells.

available *Escherichia coli* LPS, while the avirulent drug-sensitive strain ATCC 17978 cells and supernatant did not (this strain does not shed LPS [17]) (Fig. 4A). To confirm that the enhanced HUVEC permeability observed following treatment with HUMC1 supernatant was due to LPS shedding, we removed LPS using polymyxin B agarose prior to incubating HUVECs with the supernatant (Fig. S2). The removal of LPS from the HUMC1 supernatant reduced permeability to uninfected HUVEC levels (Fig. 4A), confirming the role of bacterial LPS in compromising vascular integrity.

Mice with a TLR4 mutation or TLR4 knockout mice are resistant to *A. baumannii* infection (17). Thus, we hypothesized that blocking TLR4 would abrogate the ability of *A. baumannii* to induce HUVEC permeability. Indeed, anti-TLR4 antibodies completely blocked the ability of *A. baumannii* HUMC1 or its cell-free culture supernatant to induce HUVEC permeability (Fig. 4B). Finally, by using an ARF6-GTP pulldown assay (Fig. 4C), we show that *A. baumannii* activated HUVEC ARF6 and NAV-2729 or A6-4424 reversed
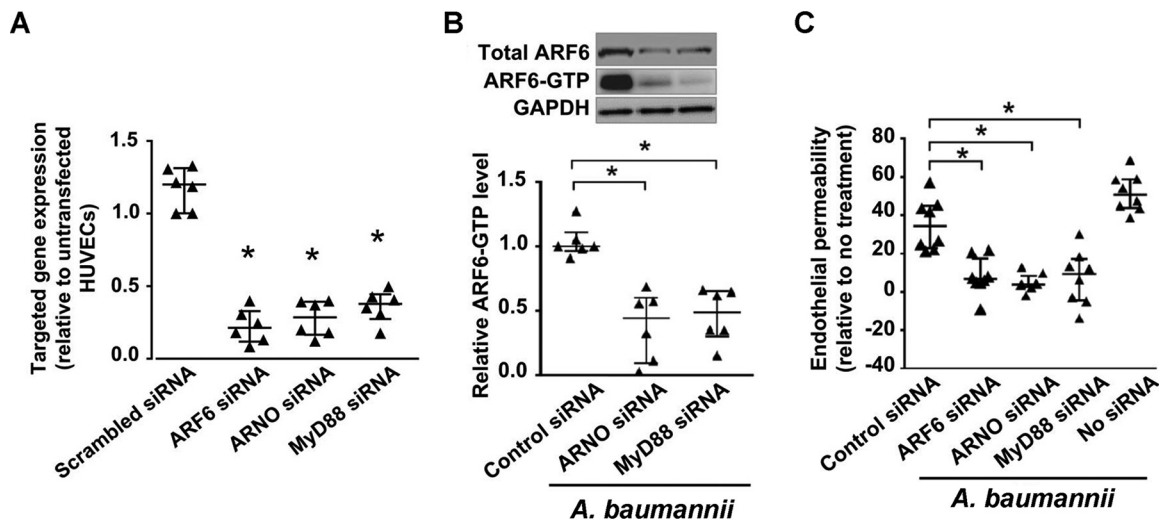
FIG 5 *A. baumannii*-mediated HUVEC permeability is induced through the MyD88/ARNO/ARF6 pathway. (A) Successful downregulation of gene expression (quantitative reverse transcription-PCR [qRT-PCR]) using siRNA constructs targeting ARF6, ARNO, or MyD88 in HUVECs. *, $P < 0.001$ versus untransfected HUVECs (2 experiments). (B and C) ARF6 expression as determined by qRT-PCR and Western blotting (B) and *A. baumannii*-mediated permeability using FITC-dextran (C) of HUVECs transfected with siRNA constructs targeting MyD88, ARNO, ARF6, or scrambled sequence (control). *, $P < 0.008$ versus control siRNA plus *A. baumannii* (B) and $P < 0.002$ versus control siRNA plus *A. baumannii* (C).

this activation and its sequelae of endothelial permeability (Fig. 4D). Similarly, A6-5093 reduced CPKP- or *P. aeruginosa*-induced HUVEC permeability (Fig. S3).

ARF6 activation can be induced by multiple mechanisms, including MyD88/ARNO (via TLR4 or the IL-1 receptor), the tumor necrosis factor (TNF) receptor, or the vascular endothelial growth factor (VEGF) receptor (12–15). Since LPS-TLR4 interactions are critical for *A. baumannii* virulence, we hypothesized that the activation of ARF6 occurs through the stimulation of the MyD88/ARNO pathway. Consequently, the downregulation of the expression of MyD88, ARNO, or ARF6 should protect HUVECs from *A. baumannii*-induced permeability. We used short interfering RNA (siRNA) targeting MyD88, ARNO, or ARF6 to detect the contribution of these proteins to *A. baumannii*-induced vascular permeability. Downregulating the expression of MyD88 or ARNO by 70 to 85% (Fig. 5A) resulted in an ~50% reduction in HUVEC ARF6-GTP levels in HUVECs infected with *A. baumannii* (Fig. 5B). As expected, transfecting HUVECs with siRNA targeting MyD88, ARNO, or ARF6 almost completely protected them from *A. baumannii*-induced permeability (Fig. 5C).

Collectively, these data show that vascular permeability is induced by GNB LPS via TLR4 activation of the MyD88/ARNO/ARF6 pathway and that ARF6 inhibitors minimize GNB-induced vascular leak *in vitro*.

A. baumannii enhances HUVEC permeability by promoting internalization of VE-cadherin. We previously showed that LPS compromises vascular integrity by the disruption of adherens junctions via internalization of VE-cadherin (13). To investigate whether a similar mechanism might be driving vascular permeability during *A. baumannii* infection, *A. baumannii* HUMC1-infected HUVECs were incubated with or without NAV-2729 and then immunostained with VE-cadherin antibody without permeabilization. *A. baumannii* reduced VE-cadherin surface expression at the cell-cell junctions (Fig. 6A) and resulted in disrupting the monolayer by 25%. In contrast, the addition of NAV-2729 to infected HUVECs preserved the surface expression of VE-cadherin and maintained the integrity of the monolayer to levels similar to those seen with uninfected HUVECs (Fig. 6A to C). Thus, *A. baumannii* compromises vascular integrity by causing VE-cadherin internalization after ARF6 activation.

Based on these data and previously published results (13–16), we propose a model of MDR GNB virulence that relies on LPS binding to TLR4, which activates two independent pathways that diverge at MyD88: (i) a pathway that activates a robust
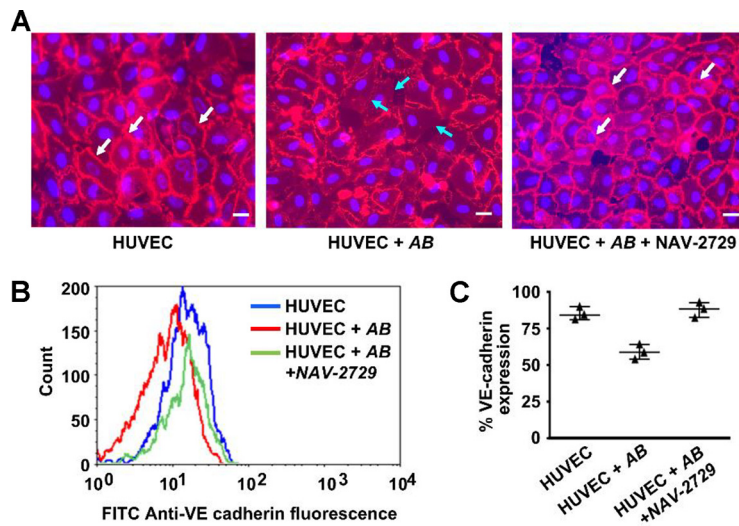
FIG 6 *A. baumannii* compromises HUVEC integrity by promoting internalization of VE-cadherin. (A) Confocal images of HUVECs incubated with *A. baumannii* HUMC1 (AB) with or without 50 μM NAV-2729 and stained with anti-VE cadherin antibody, showing a decrease in surface localization of VE-cadherin (red stain) at cell-cell junctions in the absence of NAV-2729 (cyan arrows) and restoration of junctional VE-cadherin with NAV-2729 to levels seen with uninfected HUVECs (white arrows). Cell nuclei are stained blue. Bars are 50 μM. (B and C) Representative flow cytometry staining of surface expression of VE-cadherin (B) and its quantification (C) from three independent experiments.

immune response via NF-κB, which is characterized by an increase in inflammatory cytokines, and (ii) a pathway that compromises vascular integrity via the activation of ARF6 and internalization of VE-cadherin, resulting in excessive vascular leak, tissue edema, organ failure, and death. ARF6 inhibitors block vascular leak without affecting the LPS-induced inflammatory immune response, thereby allowing the immune system to fight the infection (Fig. 7).

Population-based studies in high-income countries predicted a global burden of sepsis of $\sim$31.5 million, of which 19.4 million are classified as severe sepsis cases resulting in an estimated 5.3 million deaths annually (24). There have been >100 clinical trials to evaluate potential therapies for sepsis in the last few decades. Strategies in these trials included the use of nonselective inhibitors of inflammation (e.g., corticosteroids and nonsteroidal anti-inflammatories), neutralization of microbial mediators of sepsis, such as endotoxin, and specific inhibitors of host inflammatory mediators, such as TNF-α, IL-1, and nitric oxide. Other strategies included the use of activators of immune function (e.g., granulocyte colony-stimulating factor and interferon-γ) and the administration of anticoagulant molecules, such as activated protein C (APC), tissue factor pathway inhibitor (TFPI), anti-tissue factor antibody, anti-thrombin, thrombomodulin, or heparin (reviewed in reference 25). Despite the promising preclinical data on these targets, none of the conducted clinical trials identified a definitive treatment for sepsis. Importantly, and despite the lack of improvement in survival of sepsis patients, in aggregate these studies showed small but consistent signals of clinical benefit (25). The failure of these clinical trials could be attributed to the complexity of sepsis, because it is a dysregulated host immune response modulated by multiple factors, and targeting one molecule is unlikely to show significant benefit unless the target is known to control multiple processes that are activated during sepsis (e.g., targeting a transcription factor that controls several of the inflammatory mediators) (25, 26). Alternatively, a desirable target could be a convergent downstream effector that controls a process that is critical in worsening the outcome of sepsis, such as compromising vascular integrity (26). In this respect, the inhibition of the ARF6 molecule, which is a common convergence point in the signaling pathways of several inflammatory mediators and cytokines (e.g., LPS, TNF-α, IL-1β, and VEGF) (12, 13, 15, 16), is an attractive target in treating sepsis via maintaining vascular integrity.
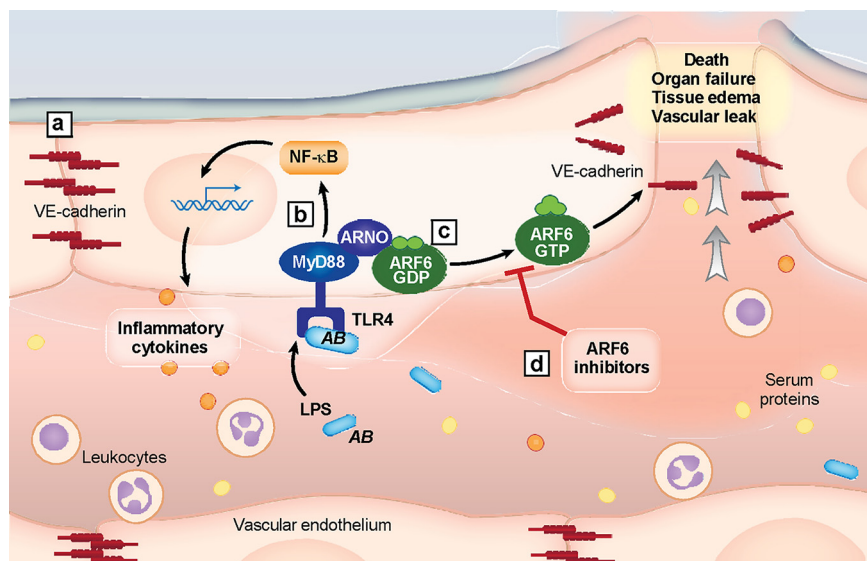
FIG 7 Model of GNB-induced vascular leak and the role of ARF6 inhibitor in preserving vascular integrity and increasing survival in bacterial infections. (A) In a normal host, the vasculature is held intact by VE-cadherin localized to the cell-cell junctions. (B) In bacterial sepsis (e.g., *A. baumannii* [AB]), LPS-induced endotoxemia triggers a robust host inflammatory response by TLR4-mediated activation of MyD88/NF-κB required for clearing the infection. (C) Bacterial LPS also triggers ARF6 activation via MyD88/ARNO, which leads to intercellular recruitment of VE-cadherin, resulting in increased vascular leak, tissue edema, organ failure, and, ultimately, death. (D) ARF6 inhibitors prevent ARF6 activation, which reduces VE-cadherin internalization, resulting in the preservation of vascular integrity without affecting the inflammatory immune response.

When designing clinical trials to evaluate potential treatments for sepsis, it is important to endeavor to recruit a homogenous cohort of patients. This process should be guided by the success and failure in preclinical models of infection. For example, in studying TNF-α as a target, preclinical models suggest that TNF neutralization in experimental sepsis is most efficacious in models of systemic endotoxemia or GNB infections, ineffective in the cecal ligation and puncture models of polymicrobial sepsis, and even harmful in experimental models of *Streptococcus pneumoniae*, *Candida*, *Listeria*, or *Mycobacterium tuberculosis* infections (25). Our results indicate that ARF6 inhibition is more likely to be effective in patients infected with GNB sepsis rather than those infected with polymicrobial organisms, since A6-5093 was marginally effective in the cecal ligation and puncture model (data not shown).

In summary, by using ARF6 inhibitors to target the vascular leak that often accompanies severe infections, we have markedly increased survival rates in preclinical models of life-threatening infections of GNB. A primary advantage of this approach is that vascular leak is a host response to infection. Therefore, targeting it should not lead to antimicrobial resistance. This approach may prove to be applicable to any infection that activates MyD88/ARF6 (e.g., *Staphylococcus aureus* and fungal infections) (27, 28). Although our data show that monotherapy can have a marked effect on survival, in practice it is more likely that such an approach would be used as adjunctive therapy to the limited drugs that are still in clinical use. Such combination therapies are the topic of active investigations.

MATERIALS AND METHODS

Organisms. *A. baumannii* HUMC1 is an MDR clinical strain with susceptibility to colistin (MIC of 2.0 μg/ml) (29). *A. baumannii* ATCC 17978 is a carbapenem-sensitive clinical strain (imipenem MIC of 0.25 μg/ml). Carbapenemase-producing *Klebsiella pneumoniae* (CPKP)-RM and *P. aeruginosa* are both MDR and were obtained from patients at Harbor-UCLA Medical Center. Organisms were grown overnight in tryptic soy broth (TSB) at 37°C with shaking. Bacterial cells were passaged for 3 h in TSB and rinsed in phosphate-buffered saline (PBS), and the final bacterial counts were determined using MacFarland standard at 600 nm. The susceptibility of the GNB to ARF6 inhibitors was assessed by the CLSI microdilution methods (30).

ARF6 inhibitors. A high-throughput screen (HTS) was used to identify direct inhibitors of ARF6. The HTS used a fluorometric biochemical assay for monitoring ARF6 activation by measuring the exchange of ARF6-bound GDP for the fluorogenic GTP-BODIPY (Life Technologies) (20). Seven distinct structural classes of ARF6 inhibitors, as well as 15 singleton hits, were identified in our HTS campaign from a library of ~50,000 commercially available compounds. We used a structural homology model of ARF6 in complex with its activator, ARNO (data not shown), to guide initial medicinal chemistry optimization for the top-priority HTS hits. The primary lead candidate series, which is based on pyrazole [1,5-a]pyrimidin-7(4H)-one scaffold], includes the original HTS hit NAV-2729 (20) along with its structural analog of A6-4424 (see Fig. S1A in the supplemental material), found via substructure searches of commercially available libraries or synthesized as part of a nascent medicinal chemistry program initiated by A6 Pharmaceuticals. A6-5093 is a highly soluble prodrug of A6-4424 designed to enhance *in vivo* administration. When A6-5093 is administered *in vivo*, its lysyl group is rapidly cleaved to produce A6-4424 (Fig. S1A and E to G).

Animal studies. (i) Conditional *Arf6* knockout mice. C57BL/6 mice harboring the *Arf6^f* (*Arf6* with flanking LoxP sites [Fig. S4A]) and *Arf6$^-$* alleles were previously described (16). Endothelium-specific *Arf6$^{-/-}$* conditional knockout mice were generated by crossing *Arf6$^{f/f}$* mice with *Arf6$^{+/-}$;Tie2-cre* mice. The excision of the *Arf6^f* allele was verified by isolating lung endothelial cells, as previously described (31), and performing Western blotting to assess ARF6 levels using anti-ARF6 antibody from Cell Signaling Technology (number 3546) (Fig. S4B).

(ii) Infection with GNB. Male ICR mice (20 to 23 g) were obtained from Envigo. Mice (ICR or *Arf6* knockout mice) were immunosuppressed using 200 mg/kg cyclophosphamide (intraperitoneal [i.p.] administration) and 250 mg/kg cortisone acetate (subcutaneous administration) on days −2 and +3 relative to infection. The current regimen results in pancytopenia for at least 9 days from the first administered dose (23). Mice were infected with aerosolized *A. baumannii* HUMC1 (18) or intratracheal instillation of CPKP (1.2×10^7 cells) or *P. aeruginosa* (2.4×10^6 cells). Treatment with ARF6 inhibitor (30 mg/kg once daily, active moiety, given i.p.) started 3 h postinfection. Infected mice treated with vehicle or those treated with 2.5 mg/kg colistin given twice daily (b.i.d.) acted as controls. All treatments continued daily for 7 days. The primary endpoints were time to morbidity. In a separate set of experiments, secondary endpoints using organs harvested on day +4 relative to infection included tissue bacterial burden by quantitative culturing, inflammatory response, and histopathological examination using hematoxylin and eosin (H&E) or Gram stain.

The inflammatory cytokine response (IL-1β, IL-6, and TNF-α) was determined using a cytometric bead array (BD Biosciences) per the manufacturer's instructions.

Mouse organ permeability was determined by injecting Evans blue dye (Sigma) 3 days after infection, harvesting organs, and processing them as previously described (12, 13).

PK studies. (i) Mouse. ARF6 inhibitor (NAV-2729 or A6-5093) was administered to male C57BL/6 mice by i.p. injection. Mice were euthanized at various times after drug administration and blood was collected. Plasma was analyzed for the presence of ARF6 inhibitor by a liquid chromatography-mass spectrometry (LC-MS) method. PK data were analyzed with Phoenix WinNonlin (Certara, Inc.).

(ii) Rat. ARF6 inhibitor (A6-5093) was administered to male Sprague-Dawley rats by intravenous (i.v.) injection given over approximately 5 s. Blood was harvested from indwelling arterial catheters at up to 10 time points over a 48-h period after drug administration. Plasma was analyzed for the presence of ARF6 inhibitor by an LC-MS method. PK data were analyzed with Phoenix WinNonlin (Certara, Inc.).

Endothelial cells. Human umbilical vein endothelial cells (HUVECs) were collected by the method of Jaffe et al. (32) and passaged twice prior to use in assays. HUVEC propagation was at 37°C in 5% CO$_2$ (33, 34). Reagents were tested for endotoxin using a chromogenic *Limulus* amebocyte lysate assay (Charles River Laboratories), and the endotoxin concentrations were <0.01 IU/ml.

Transwell permeability assay. HUVECs were seeded on 0.4-μm transwell inserts (Corning) coated with fibronectin (10 to 15 μg/ml in PBS) and fitted in 24-well plates (Costar). HUVECs were grown to confluence in M-199 medium without phenol red and then challenged with 10^7 bacterial cells for 3 h at 37°C. Following incubation, 3 μl of 50-mg/ml fluorescein isothiocyanate (FITC)-dextran-10K (Sigma) was added to the top chamber, and the amount of vascular leak was determined 1 h later by quantifying the concentration of the dye in the bottom chamber using a fluorescence microplate reader at 488 nm.

To investigate the effects of stimuli or inhibitors on HUVEC permeability, the assay was repeated with or without 50 μM ARF6 inhibitors (A6 Pharmaceuticals), 50 μg/ml anti-TLR4 antibody or isotype control antibody (BioLegend), or 100 ng/ml *E. coli* LPS. To deplete bacterial supernatant of any shed LPS, supernatants were treated with polymyxin B agarose beads.

ARF6 pulldown assays. HUVECs were treated with *A. baumannii* HUMC1 with or without 50 μM ARF6 inhibitor for 4 h. The cells were washed with ice-cold PBS and lysed with ice-cold lysis buffer supplemented with protease and phosphatase inhibitor (number 26186; Thermo Scientific). Immunoprecipitation was performed with glutathione *S*-transferase (GST)-GGA3-conjugated agarose beads (Cell Biolabs) (13). Protein levels of GTP-bound ARF6 and total ARF6 in cell lysates were detected by Western blotting with an anti-ARF6 antibody (1:1,000 in 5% milk) (Sigma).

HUVEC gene knockdown. HUVECs were trypsinized and resuspended in growth medium with 30 nM siRNAs targeting MyD88 (SI00300909), ARNO (SI00061299), and ARF6 (SI02757286) using HiPerFect transfection reagent (Qiagen) (13) and incubated for 2 days at 37°C. The transfection process was repeated once more. All-Stars negative-control siRNA (Qiagen) was used as a control. RNA from transfected HUVEC was isolated using an RNeasy Plus minikit (Qiagen) after incubation for 4 h with or without *A. baumannii* HUMC1. cDNA was synthesized using a RETROscript reverse transcription kit (Thermo Fisher Scientific). Quantitative PCR (qPCR) was prepared with TaqMan gene expression assay

probes (Thermo Fisher Scientific) and TaqMan gene expression master mix (Thermo Fisher Scientific). The qPCR was carried out with a thermal-cycling program with the following steps: initial denaturing step for 10 min at 95°C, followed by 40 cycles of denaturing at 95°C for 15 s and then annealing/elongation at 60°C for 1 min. A human 18S rRNA gene probe (Hs00917508_m1) was used as a reference control. Real-time probes of targeted genes were human ARF6 (Hs01922781_g1), MyD88 (Hs00851874_g1), and ARNO (Hs00244669_m1). The comparative threshold cycle ($\Delta\Delta C_T$) method was used for data analysis.

VE-cadherin expression by confocal microscopy. HUVECs were seeded on coverslips that had been precoated with fibronectin in 24-well plates. HUVECs were incubated with *A. baumannii* HUMC1 for 4 h with or without 50 μM ARF6 inhibitor, washed twice with PBS, and fixed with 4% formaldehyde for 10 min. The cells were washed 4 times with PBS and then blocked with 300 μl 50% human AB serum (Sigma) for 10 min at room temperature. Mouse monoclonal VE-cadherin antibody (number 555661; BD Biosciences) was added to the HUVECs (2.5 μg/ml) and held overnight at 4°C. HUVECs then were washed with PBS and counterstained with 2 mg/ml Alexa Fluor 594 F(ab')2 goat anti-mouse IgG (1:300 in 2% human serum–PBS; Thermo Fisher Scientific) for 1 h at room temperature. The cells were stained with 1 μg/ml Hoechst 33342 (ThermoFisher) in PBS for 10 min. HUVECs were washed twice with distilled water and wet mounted on glass slides before being examined by confocal microscopy.

VE-cadherin quantification by flow cytometry. HUVECs were seeded in 6-well plates (Costar) precoated with fibronectin. HUVECs were incubated with *A. baumannii* HUMC1 for 4 h with or without 50 μM ARF6 inhibitor and then washed twice with PBS. HUVECs were detached from the plate with CellStripper dissociation reagent (ThermoFisher) that had been prewarmed at 37°C for 10 min. M199 medium containing 20% fetal bovine serum was added to each well and the cells collected. HUVECs were centrifuged, washed with PBS, and then fixed with 0.5 ml of 4% formaldehyde at room temperature for 15 min. The fixed cells were washed with PBS, blocked with 50% human AB serum, and then incubated with 2.5 μg/ml mouse monoclonal VE-cadherin antibody (number 555661; BD Biosciences) overnight at 4°C. The next day, cells were washed with PBS and then incubated with Alexa Fluor 488 F(ab')2 goat anti-mouse IgG secondary (ThermoFisher) (1:300 in 2% human serum–PBS from a stock of 2 mg/ml) for 1 h at 4°C. Cells were washed 3 times with 2% serum–PBS, and the cells were transferred to fluorescence-activated cell sorter (FACS) tubes. The fluorescence of VE-cadherin was quantified by using a FACSCalibur (Becton, Dickinson) instrument equipped with an argon laser emitting at 488 nm. Fluorescence data (10^4 events) were collected with logarithmic amplifiers, and percent fluorescence was calculated using CellQuest software.

Ethics statement. All procedures involving mice were approved by the IACUC of the Lundquist Institute for Biomedical Innovations at Harbor-UCLA Medical Center (protocol number 30449) according to the NIH guidelines for animal housing and care. Mice determined to be moribund according to detailed and well-characterized criteria were euthanized by pentobarbital overdose, followed by cervical dislocation.

Statistical analysis. Each *in vitro* experiment was carried out in triplicate, and the experiment was repeated at least twice. Survival was compared by nonparametric log rank. Categorical variables were compared using the Mann-Whitney U test for unpaired comparisons. A *P* value of <0.05 was considered significant.

SUPPLEMENTAL MATERIAL

Supplemental material is available online only.
SUPPLEMENTAL FILE 1, PDF file, 1 MB.

REFERENCES

1. Tacconelli E, WHO Pathogens Priority List Working Group. 2018. Discovery, research, and development of new antibiotics: the WHO priority list of antibiotic-resistant bacteria and tuberculosis. Lancet Infect Dis 18:318–327. https://doi.org/10.1016/S1473-3099(17)30753-3.

2. Magill SS, Emerging Infections Program Healthcare-Associated Infections and Antimicrobial Use Prevalence Survey Team, Edwards JR, Bamberg W, Beldavs ZG, Dumyati G, Kainer MA, Lynfield R, Maloney M, McAllister-Hollod L, Nadle J, Ray SM, Thompson DL, Wilson LE, Fridkin SK. 2014. Multistate point-prevalence survey of health care-associated infections. N Engl J Med 370:1198–1208. https://doi.org/10.1056/NEJMoa1306801.

3. Maragakis LL, Tucker MG, Miller RG, Carroll KC, Perl TM. 2008. Incidence and prevalence of multidrug-resistant Acinetobacter using targeted active surveillance cultures. JAMA 299:2513–2514. https://doi.org/10.1001/jama.299.21.2513.

4. Paterson DL. 2006. The epidemiological profile of infections with multidrug-resistant Pseudomonas aeruginosa and Acinetobacter species. Clin Infect Dis 43(Suppl 2):S43–S48. https://doi.org/10.1086/504476.

5. Matthay MA, Ware LB, Zimmerman GA. 2012. The acute respiratory distress syndrome. J Clin Investig 122:2731–2740. https://doi.org/10.1172/JCI60331.

6. Bisbe J, Gatell JM, Puig J, Mallolas J, Martinez JA, Jimenez de Anta MT, Soriano E. 1988. Pseudomonas aeruginosa bacteremia: univariate and multivariate analyses of factors influencing the prognosis in 133 episodes. Rev Infect Dis 10:629–635. https://doi.org/10.1093/clinids/10.3.629.

7. Fraenkel-Wandel Y, Raveh-Brawer D, Wiener-Well Y, Yinnon AM, Assous MV. 2016. Mortality due to blaKPC Klebsiella pneumoniae bacteraemia. J Antimicrob Chemother 71:1083–1087. https://doi.org/10.1093/jac/dkv414.

8. Lautenbach E, Synnestvedt M, Weiner MG, Bilker WB, Vo L, Schein J, Kim M. 2009. Epidemiology and impact of imipenem resistance in Acinetobacter baumannii. Infect Control Hosp Epidemiol 30:1186–1192. https://doi.org/10.1086/648450.

9. ARDS Definition Task Force, Ranieri VM, Rubenfeld GD, Thompson BT, Ferguson ND, Caldwell E, Fan E, Camporota L, Slutsky AS. 2012. Acute respiratory distress syndrome: the Berlin definition. JAMA 307:2526–2533. https://doi.org/10.1001/jama.2012.5669.

10. Lee NY, Chang TC, Wu CJ, Chang CM, Lee HC, Chen PL, Lee CC, Ko NY, Ko WC. 2010. Clinical manifestations, antimicrobial therapy, and prognostic factors of monomicrobial Acinetobacter baumannii complex bacteremia. J Infect 61:219–227. https://doi.org/10.1016/j.jinf.2010.07.002.

11. Matthay MA, Zimmerman GA. 2005. Acute lung injury and the acute respiratory distress syndrome: four decades of inquiry into pathogenesis and rational management. Am J Respir Cell Mol Biol 33:319–327. https://doi.org/10.1165/rcmb.F305.

12. London NR, Zhu W, Bozza FA, Smith MC, Greif DM, Sorensen LK, Chen L, Kaminoh Y, Chan AC, Passi SF, Day CW, Barnard DL, Zimmerman GA, Krasnow MA, Li DY. 2010. Targeting Robo4-dependent Slit signaling to survive the cytokine storm in sepsis and influenza. Sci Transl Med 2:23ra19. https://doi.org/10.1126/scitranslmed.3000678.

13. Davis CT, Zhu W, Gibson CC, Bowman-Kirigin JA, Sorensen L, Ling J, Sun H, Navankasattusas S, Li DY. 2014. ARF6 inhibition stabilizes the vasculature and enhances survival during endotoxic shock. J Immunol 192:6045–6052. https://doi.org/10.4049/jimmunol.1400309.

14. Jones CA, Nishiya N, London NR, Zhu W, Sorensen LK, Chan AC, Lim CJ, Chen H, Zhang Q, Schultz PG, Hayallah AM, Thomas KR, Famulok M, Zhang K, Ginsberg MH, Li DY. 2009. Slit2-Robo4 signalling promotes vascular stability by blocking Arf6 activity. Nat Cell Biol 11:1325–1331. https://doi.org/10.1038/ncb1976.

15. Zhu W, London NR, Gibson CC, Davis CT, Tong Z, Sorensen LK, Shi DS, Guo J, Smith MC, Grossmann AH, Thomas KR, Li DY. 2012. Interleukin receptor activates a MYD88-ARNO-ARF6 cascade to disrupt vascular stability. Nature 492:252–255. https://doi.org/10.1038/nature11603.

16. Zhu W, Shi DS, Winter JM, Rich BE, Tong Z, Sorensen LK, Zhao H, Huang Y, Tai Z, Mleynek TM, Yoo JH, Dunn C, Ling J, Bergquist JA, Richards JR, Jiang A, Lesniewski LA, Hartnett ME, Ward DM, Mueller AL, Ostanin K, Thomas KR, Odelberg SJ, Li DY. 2017. Small GTPase ARF6 controls VEGFR2 trafficking and signaling in diabetic retinopathy. J Clin Investig 127:4569–4582. https://doi.org/10.1172/JCI91770.

17. Lin L, Tan B, Pantapalangkoor P, Ho T, Baquir B, Tomaras A, Montgomery JI, Reilly U, Barbacci EG, Hujer K, Bonomo RA, Fernandez L, Hancock RE, Adams MD, French SW, Buslon VS, Spellberg B. 2012. Inhibition of LpxC protects mice from resistant Acinetobacter baumannii by modulating inflammation and enhancing phagocytosis. mBio 3:e00312-12. https://doi.org/10.1128/mBio.00312-12.

18. Luo G, Spellberg B, Gebremariam T, Bolaris M, Lee H, Fu Y, French SW, Ibrahim AS. 2012. Diabetic murine models for Acinetobacter baumannii infection. J Antimicrob Chemother 67:1439–1445. https://doi.org/10.1093/jac/dks050.

19. Uppuluri P, Lin L, Alqarihi A, Luo G, Youssef EG, Alkhazraji S, Yount NY, Ibrahim BA, Bolaris MA, Edwards JE, Jr, Swidergall M, Filler SG, Yeaman MR, Ibrahim AS. 2018. The Hyr1 protein from the fungus Candida albicans is a cross kingdom immunotherapeutic target for Acinetobacter bacterial infection. PLoS Pathog 14:e1007056. https://doi.org/10.1371/journal.ppat.1007056.

20. Yoo JH, Shi DS, Grossmann AH, Sorensen LK, Tong Z, Mleynek TM, Rogers A, Zhu W, Richards JR, Winter JM, Zhu J, Dunn C, Bajji A, Shenderovich M, Mueller AL, Woodman SE, Harbour JW, Thomas KR, Odelberg SJ, Ostanin K, Li DY. 2016. ARF6 is an actionable node that orchestrates oncogenic GNAQ signaling in uveal melanoma. Cancer Cell 29:889–904. https://doi.org/10.1016/j.ccell.2016.04.015.

21. Li J, Nation RL, Milne RW, Turnidge JD, Coulthard K. 2005. Evaluation of colistin as an agent against multi-resistant Gram-negative bacteria. Int J Antimicrob Agents 25:11–25. https://doi.org/10.1016/j.ijantimicag.2004.10.001.

22. Boucher HW, Talbot GH, Bradley JS, Edwards JE, Gilbert D, Rice LB, Scheld M, Spellberg B, Bartlett J. 2009. Bad bugs, no drugs: no ESKAPE! An update from the Infectious Diseases Society of America. Clin Infect Dis 48:1–12. https://doi.org/10.1086/595011.

23. Sheppard DC, Rieg G, Chiang LY, Filler SG, Edwards JE, Jr, Ibrahim AS. 2004. Novel inhalational murine model of invasive pulmonary aspergillosis. Antimicrob Agents Chemother 48:1908–1911. https://doi.org/10.1128/aac.48.5.1908-1911.2004.

24. Fleischmann C, International Forum of Acute Care Trialists, Scherag A, Adhikari NKJ, Hartog CS, Tsaganos T, Schlattmann P, Angus DC, Reinhart K. 2016. Assessment of global incidence and mortality of hospital-treated sepsis. Current estimates and limitations. Am J Respir Crit Care Med 193:259–272. https://doi.org/10.1164/rccm.201504-0781OC.

25. Marshall JC. 2014. Why have clinical trials in sepsis failed? Trends Mol Med 20:195–203. https://doi.org/10.1016/j.molmed.2014.01.007.

26. van der Poll T, van de Veerdonk FL, Scicluna BP, Netea MG. 2017. The immunopathology of sepsis and potential therapeutic targets. Nat Rev Immunol 17:407–420. https://doi.org/10.1038/nri.2017.36.

27. Feuerstein R, Seidl M, Prinz M, Henneke P. 2015. MyD88 in macrophages is critical for abscess resolution in staphylococcal skin infection. J Immunol 194:2735–2745. https://doi.org/10.4049/jimmunol.1402566.

28. Haley K, Igyártó BZ, Ortner D, Bobr A, Kashem S, Schenten D, Kaplan DH. 2012. Langerhans cells require MyD88-dependent signals for Candida albicans response but not for contact hypersensitivity or migration. J Immunol 188:4334–4339. https://doi.org/10.4049/jimmunol.1102759.

29. Luo G, Lin L, Ibrahim AS, Baquir B, Pantapalangkoor P, Bonomo RA, Doi Y, Adams MD, Russo TA, Spellberg B. 2012. Active and passive immunization protects against lethal, extreme drug resistant-Acinetobacter baumannii infection. PLoS One 7:e29446. https://doi.org/10.1371/journal.pone.0029446.

30. CLSI. 2009. Methods for dilution antimicrobial susceptibility tests for bacteria that grow aerobically. CLSI, Wayne, PA.

31. Jones CA, London NR, Chen H, Park KW, Sauvaget D, Stockton RA, Wythe JD, Suh W, Larrieu-Lahargue F, Mukouyama Y-S, Lindblom P, Seth P, Frias A, Nishiya N, Ginsberg MH, Gerhardt H, Zhang K, Li DY. 2008. Robo4 stabilizes the vascular network by inhibiting pathologic angiogenesis and endothelial hyperpermeability. Nat Med 14:448–453. https://doi.org/10.1038/nm1742.

32. Jaffe EA, Nachman RL, Becker CG, Minick CR. 1973. Culture of human endothelial cells derived from umbilical veins. Identification by morphologic and immunologic criteria. J Clin Investig 52:2745–2756. https://doi.org/10.1172/JCI107470.

33. Gebremariam T, Lin L, Liu M, Kontoyiannis DP, French S, Edwards JE, Jr, Filler SG, Ibrahim AS. 2016. Bicarbonate correction of ketoacidosis alters host-pathogen interactions and alleviates mucormycosis. J Clin Investig 126:2280–2294. https://doi.org/10.1172/JCI82744.

34. Gebremariam T, Liu M, Luo G, Bruno V, Phan QT, Waring AJ, Edwards JE, Jr, Filler SG, Yeaman MR, Ibrahim AS. 2014. CotH3 mediates fungal invasion of host cells during mucormycosis. J Clin Investig 124:237–250. https://doi.org/10.1172/JCI71349.